Journal of Materials Chemistry C

PAPER

View Article Online
View Journal | View Issue

Cite this: J. Mater. Chem. C, 2015, 3, 11945

Self-assembly of tetra(aniline) nanowires in acidic aqueous media with ultrasonic irradiation†

Wei Lyu,[ab] Jiangtao Feng,[a] Wei Yan*[ab] and Charl FJ Faul*[c]

Received 13th July 2015,
Accepted 24th October 2015

DOI: 10.1039/c5tc02093j

www.rsc.org/MaterialsC

An environmentally friendly method is developed to explore the self-assembly of Ph/NH_2-capped tetra(aniline), **TANI**, nanowires in acidic aqueous media with ultrasonic irradiation. Ultrasonic irradiation is demonstrated to be an effective method to achieve self-assembled thermodynamic equilibrium for nanostructure formation in only 2 minutes. Further assembly, *i.e.*, the formation of thicker **TANI** nanowires in acidic solution left undisturbed for 96 h without the addition of any organic solvent, is also investigated. The self-assembly behaviour of **TANI** is studied using FT-IR, Raman, UV-Vis spectroscopy, thermogravimetric analysis, X-ray diffraction, and scanning electron microscopy. Investigations suggest that extra hydrogen bonding associated with the protonation, electrostatic interactions and π–π stacking interaction are important for the self-organization of **TANI** nanowires. Furthermore, the assembly behaviour of **TANI** nanowires is dependent on the properties of the dopant, including size and concentration, and reflected in the conductivity of the assembled structures. These results provide insight to understand and tune the self-assembly behaviour of nanostructured oligo(aniline)s in complex dopant-containing systems, and form the basis for further detailed mechanistic studies.

1. Introduction

Oligo(aniline)s, a class of organic semiconductors, have attracted growing interest in recent years because of their unique redox properties and relatively high conductivity,[1] good solubility and excellent processability,[2] and potential use in many applications.[3–10] Additionally, they possess well-defined chemical structures and offer opportunities for molecular engineering and designing oligo(aniline)s-based organic (semi)conductors with defined architectures, functionalities and properties.[11–15] Among the oligo(aniline)s, phenyl/amine-capped tetra(aniline) (**TANI**), the shortest oligomer representing the emeraldine oxidation state, is an important model compound for poly(aniline) (**PANI**).[1]

Recently, a number of reports have indicated that oligo(aniline)s, as a class of π-conjugated molecules, can self-assemble into well-defined nano- and hierarchical microstructures by intermolecular interactions such as hydrogen bonds, π–π stacking, ionic interactions and hydrophobic interactions.[13,14,16–21] Controlled aggregation of oligo(aniline) molecules through π–π stacking interactions and hydrogen bonding in a mixture of ethanol and aqueous inorganic dopant acid led to the formation of diverse structures, including nanowires, nanoribbons, rectangular nanoplates and nanoflowers.[1,14] Short nanofibers were also obtained through π–π stacking interactions and hydrogen bonding by a similar method.[22] With the aim to uncover the self-assembly mechanism of nanostructured oligo(aniline)s in complex systems in a methodical fashion, it is necessary and desirable to carefully consider the self-assembly behaviour of oligo(aniline)s in solely inorganic acidic aqueous media (*i.e.*, in the absence of any organic additives or solvents, and defined and described as "acidic media" in the rest of the manuscript). Once these mechanisms are clarified, the formation mechanism and geometry of more complex nanostructures, through the addition of organic solvents, can be addressed.[23,24] Previous studies indicated that only poorly defined structures were obtained in acidic media (formed at low concentration and left undisturbed for 4–5 days).[1] However, keeping other related studies in mind,[25] such systems with slow dynamics due to low solubility might not have reached their thermodynamic stable states and thus do not show optimized structures. We therefore decided to explore new routes to attempt to reach equilibrium within the constraints provided by acidic media.

It is well known that oscillatory pressure and intensities can be induced by the propagation of ultrasound in a liquid, resulting in the phenomenon of cavitation. During cavitation it is claimed that bubble collapse produces a temperature of roughly 5000 °C, a pressure of about 1000 atm, and heating/cooling rates above 10^{10} K s^{-1}. It is expected that this environment could facilitate the rapid and effective self-assembly of **TANI**.[26]

[a] Department of Environmental Science and Engineering, Xi'an Jiaotong University, Xi'an 710049, P. R. China. E-mail: yanwei@xjtu.edu.cn; Fax: +86-029-82664731; Tel: +86-029-82664731
[b] State Key Laboratory of Multiphase Flow in Power Engineering, Xi'an Jiaotong University, Xi'an, 710049, P. R. China
[c] School of Chemistry, University of Bristol, BS8 1TS, Bristol, UK. E-mail: charl.faul@bristol.ac.uk

† Electronic supplementary information (ESI) available. See DOI: 10.1039/c5tc02093j

We therefore adopted sonication to investigate the self-assembly behaviour of **TANI** in acidic media. A possible self-assembly mechanism for **TANI** nanowires and the driving forces are postulated. The further assembly behaviour and the formation of thicker nanowires at different acid concentrations are also studied.

2. Experimental

2.1. Synthesis

N-phenyl-1,4-phenylenediamine was purchased from Aldrich Chemical Co. Ltd and other chemicals were from Tianli Chemical Reagent Co. Ltd. All chemicals were used as received. The synthesis of **TANI** was performed following published literature procedures.[18,19] In a typical procedure, ferric chloride hexahydrate (2.70 g, 10.0 mmol) in HCl solution (10 ml, 0.1 M) was rapidly added to a solution of the hydrochloride salt of *N*-phenyl-1,4-phenylenediamine (dianiline salt, 2.56 g, 10.0 mmol) suspended in HCl solution (50 ml, 0.1 M). After vigorous mechanical stirring for 2 h, the product was collected by centrifugation and washed repeatedly with 0.1 M HCl until the supernatant became clear. The precipitate was purified by Soxhlet extraction with acetone for 12 h to remove any residual dianiline salt. The resulting precipitate, labelled as Ph/NH_2-capped tetra(aniline), **TANI**, in the emeraldine salt state (**TANI**-ES), was then treated with a mixture of ammonium hydroxide solution (2 M, 50 ml) and acetone (300 ml) for 30 min. The acetone was then removed under reduced pressure. The precipitate was collected by centrifugation and dried in a vacuum oven at 50 °C for 48 h to yield **TANI** in the emeraldine base state, **TANI**-EB (yield: 49.8%). MALDI-TOF-MS: *m*/*z* calculated for $C_{24}H_{20}N_4$ = 366. Found 366.14. FTIR (KBr, cm^{-1}): 3373 (s, ν_{N-H}), 3023 (m, ν_{C-H}), 1593 (s, $\nu_{C=C}$ of quinone rings), 1502 (s, $\nu_{C=C}$ of benzenoid rings), 1301 (s, ν_{C-N}), 815 (m, δ_{C-H}), 746 (m, δ_{C-H}). EA Calcd for $C_{24}H_{20}N_4$: C 83.7, N 16.3. Found: C 84.9, N 15.1%.

2.2. Preparation of nanowires

In a typical procedure, **TANI**-EB powder (4 mg) was added to 20 ml HCl aqueous solution of different concentrations (0.1 M, 1 M, 5 M, 7 M) under ultrasonic irradiation for 2 min with the ultrasonic power and frequency set at 200 W and 59 kHz. In this study, the doped **TANI** samples are labelled as US-0.1M, US-1M, US-5M and US-7M, respectively. The mixtures were then left undisturbed for 96 h and labelled as UE-0.1M, UE-1M, UE-5M and UE-7M, respectively. Table 1 displays the elemental analysis (C, N, Cl) of all samples and the molecular formula. Fully doped **TANI**-ES is expected to show a Cl/N ratio of 0.5. The corresponding energy dispersive X-ray (EDS) spectra are shown in ESI,† Fig. S1.

2.3. Preparation of the US-5M and TANI-ES modified carbon paste electrode (CPE)

The modified CPE was prepared by thorough hand-mixing of high purity graphite powder (99.98%, Sinopharm Chemical reagent Co, Ltd), silicone oil (Sinopharm Chemical reagent Co, Ltd) and sample (US-5M or **TANI**-ES) powder in a ratio of 60 : 30 : 10 (w/w) in an agate mortar, using a pestle to obtain a homogeneous paste in 15 min. A portion of the homogeneous paste was packed into a glass tube with $\Phi = 5 \times 1$ mm with a copper wire as the electrical contact with the external circuit.

Table 1 Elemental analysis of HCl-doped **TANI** samples, their molecular formula and Cl/N ratio

Samples	%C	%N	%Cl	Molecular formula	Cl/N
TANI-HCl (calc)[a]	80.0	13.3	6.70	$C_{24}H_{18}N_4{\cdot}2HCl$	0.50
TANI-ES	80.1	13.4	6.50	$C_{24}H_{18}N_4{\cdot}2HCl$	0.49
US-0.1M	79.9	13.3	6.80	$C_{24}H_{18}N_4{\cdot}2HCl$	0.51
US-1M	76.7	12.8	10.5	$C_{24}H_{18}N_4{\cdot}3.3HCl$	0.82
US-5M	77.0	12.8	10.2	$C_{24}H_{18}N_4{\cdot}3.3HCl$	0.80
US-7M	80.1	13.3	6.60	$C_{24}H_{18}N_4{\cdot}2HCl$	0.50

[a] The values for tetra(aniline) are calculated values for HCl-doped **TANI**.

2.4. Characterization

Samples for scanning electron microscope (SEM) studies were prepared by depositing 1 to 2 drops of the dispersion onto a silicon substrate. SEM images were taken with a JEOL JSM-6700 Field Emission Scanning Electron Microscope. The elemental analysis was performed on a JEOL JSM-6460 Field Emission Scanning Electron Microscope equipped with an energy dispersive spectrometer (EDS). The average diameters of nanowires were measured by Image-Pro Plus 6.0 imaging software. FT-IR spectra of the dried samples were obtained on a Bruker, TENSOR37 infrared spectrometer with KBr pellets. Raman spectra at 632.8 nm excitation radiation were acquired on a HORIBA JOBIN YVON HR 800 spectrometer. Cyclic voltammetry (CV) was investigated on a CHI 660D electrochemical work-station with a conventional three electrode cell, using Ag/AgCl (3 M KCl) as the reference electrode and Pt foil as the counter electrode. The working electrode was the modified CPE. CV investigations were carried out in 1.0 M sulfuric acid solution (degassed for 30 minutes with high purity N_2 before use) in the range from −0.2 to 1.0 V at a scan rate of 50 mV s^{-1}. UV-Vis spectra were recorded on an Agilent 8453 instrument. Samples were shaken very gently before the UV-Vis spectra were recorded. Thermogravimetric analysis (TG) measurements were performed on a Setaram Labsys Evo TG-DSCS-TYPE DSC sensor at a heating rate of 10 °C min^{-1} from room temperature to 800 °C under steady nitrogen flow. Powder X-ray diffraction (XRD) patterns of the UE samples nanostructures were taken on an X'pert MPDPro (PANalytical Co.) diffractometer using Cu Kα radiation (40 kV, 40 mA) with a scan rate of 5 deg min^{-1}. XRD patterns of the US samples nanostructures were taken on a Rigaku Dmax-RA with a scan rate of 4 deg min^{-1}. Electronic transport properties of pressed pellets from the obtained **TANI** nanowires were performed using a four-probe measurement (RTS-4 four probe meter) in order to determine the conductivities of these nanostructures.

3. Results and discussion

TANI, synthesized according to previously reported methods, possessed a granular, agglomerated morphology (Fig. 1a).[1,18,19] However, we found that nanostructures of **TANI** can be grown

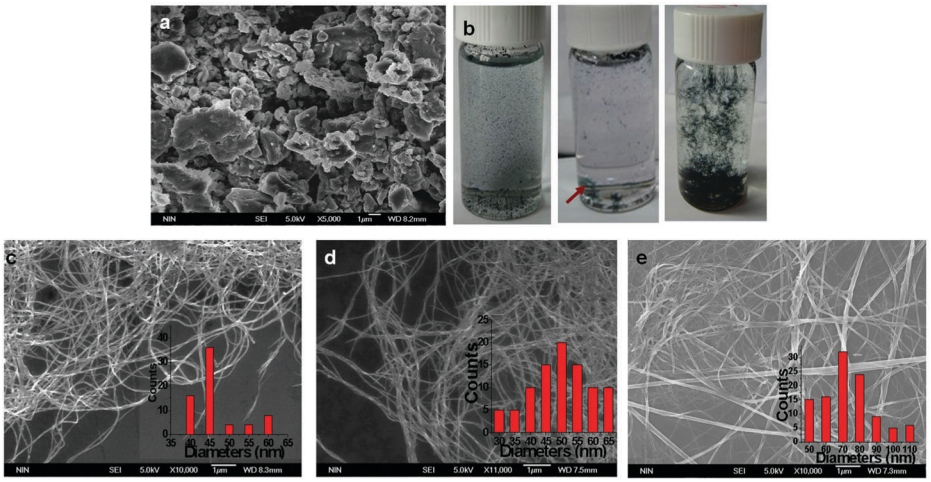

Fig. 1 (a) A SEM image of the as-synthesized **TANI**-EB powder. (b) Micrographs show a mixture of **TANI**-EB and 5 M HCl at the beginning of the process (left vial), at the end of 7 days' standing without ultrasonic irradiation (middle vial), and the green **TANI** nanowire dispersion created under ultrasonic irradiation (right vial, US-5M). (c) A SEM image of a network of US-5M nanowires created with ultrasonic irradiation. (d) A SEM image of the nanowires obtained at the end of 7 days' standing without ultrasonic irradiation. (e) A SEM image of thicker nanowires obtained 96 h after ultrasonic irradiation (UE-5M). Histogram values were obtained by measuring the nanowire diameters in Fig. 1c–e inserts.

by adding this granular powder to a 5 M HCl aqueous solution followed by ultrasonic irradiation for just 2 min (Fig. 1b, right vial). A SEM image of the resultant sample shows that long nanowires with high aspect ratios are created during this process (Fig. 1c). The nanowires typically range in diameter from 30 to 60 nm and are up to hundreds of micrometers long. If these nanowires are then left undisturbed for 96 h, thicker nanowires with an average diameter of 73 nm are obtained (Fig. 1e). Moreover, there was no obvious change in the obtained **TANI** nanowires with varying ultrasonic irradiation time and power (Fig. S2, ESI†).

In order to confirm that sonication is an effective route to thermodynamically stable self-assembled **TANI** nanostructures, (here in 5 M HCl aqueous solution), a control experiment of the same system without ultrasonic irradiation was left undisturbed for 7 days, in an attempt to reach equilibrium. It can be seen from Fig. 1b (middle vial) and Fig. 1d, a small amount of nanowires with an average diameter of 50 nm, similar to those obtained with ultrasonic irradiation for 2 min (Fig. 1c), was formed. Considering the short irradiation time, ultrasonic irradiation obviously accelerated the formation of nanowires and enabled the system to reach a thermodynamic stable state much more quickly when compared with the non-sonicated system.[27]

As-synthesized **TANI**-EB (with an agglomerated morphology), undergoes a transformation into well-defined nanowires of the protonated emeraldine salt **TANI**-ES state. As neither **TANI**-EB nor **TANI**-ES is water soluble, we expect that a solid–solid phase transformation, aided by the ultrasonic irradiation, leads to the formation of the found morphologies. Reversible non-covalent interactions such as hydrogen bonding and π–π stacking have been proposed as the driving force to regulate supramolecular organization.[14,16,17] It was found that, when dialyzing the well-defined **TANI**-ES nanostructure with $NH_3{\cdot}H_2O$, an agglomerated morphology is obtained again (see Fig. S3, ESI†). To the best of our knowledge, no work has been reported on the solid–solid phase transformations of **TANI** or poly(aniline). We are currently performing time-dependent electron microscopy studies in our laboratories to clarify the exact nature and details of this suspected "nucleation-and-growth" mechanism.

A control experiment, in which **TANI**-EB powder was added to deionized water with ultrasonic irradiation for 2 min, was also carried out; no well-defined nanostructures were obtained (Fig. S4, ESI†), leading us to conclude that, the self-assembly and formation of the **TANI** nanowires is highly dependent on the combination of the dopant acid and ultrasonic irradiation.

Colomban *et al.* investigated the spectroscopy of the pronated forms of **PANI** and interpreted broad infrared absorption centered near 1100 cm^{-1} and cut by numerous negative bands (Evans holes) as NH stretching bands of a strong asymmetric interchain $NH^+\cdots N$ hydrogen bond.[28] They pointed out that the $NH^+\cdots N$ hydrogen bonds led to interchain conversions, which can generate charge carriers. In other words, $NH^+\cdots N$ hydrogen bonds associated with the protonation process, where the oxidation level is equal to 50%, always exists in the ES state. However, few reports have paid attention to such interactions.

Here, combined with the results of our control experiments, we propose that this extra hydrogen bonding associated with the protonation process is one of the important driving forces for the nanowires assembly.[1] We examined the spectroscopic data of **TANI**-EB and US-5M samples. As can be seen in Fig. 3c, the broad absorption extending from 1800 to 400 cm^{-1} in the infrared spectra of US-5M exhibits Evans holes. These narrow bands also appear at the same or very similar frequency in the Raman spectra (see Fig. 3d and Table S1, ESI†), indicating the existence of $NH^+\cdots N$ hydrogen bonds between molecular chains for this overdoped sample, as shown in Fig. 2.

In terms of **TANI**-ES, some weak Evans holes could also be observed in the infrared spectra (Fig. 3b) of this nominally fully doped sample. We note that a few short nanowires, which might be assembled by the same driving force as for US-5M, exist in the bulk of irregularly shaped **TANI**-ES structures, as

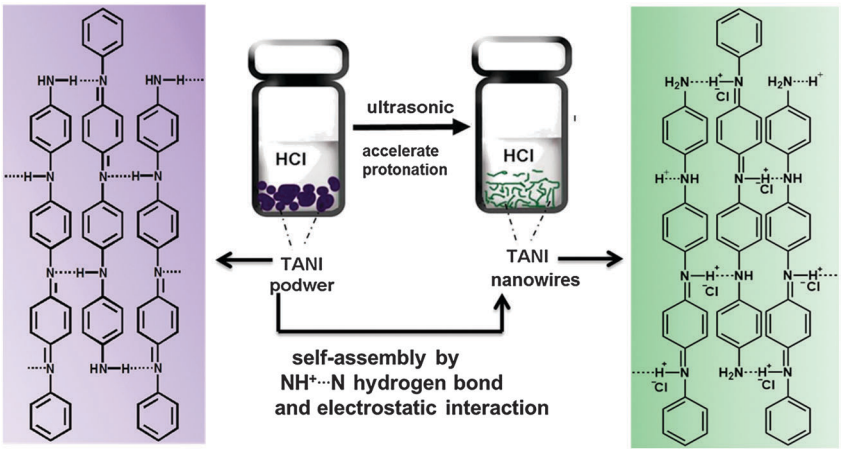

Fig. 2 Schematic showing potential hydrogen-bonding interactions in the formation of **TANI** nanowires.

seen in Fig. S5 (ESI†). Similar to bulk conventional agglomerated **PANI**, which seems to have an intrinsically nanofibers morphology, the amorphous secondary growth that agglomerates onto the nanofibers leads to the irregularly shaped morphology.[29]

Moreover, the electrostatic interactions introduced by the dopants can also serve as a further driving force for self-assembly.[2] In this system, it was found that the formation of nanostructures is related to the size of the dopant acid molecules (*i.e.* the counterion size): smaller dopants such as HNO_3 and HCl can promote the assembly and formation of nanowires, while larger dopant counterions such as SO_4^{2-}, PO_4^{2-}, camphorsulfonate ($C_{10}H_{15}OSO_3^-$, from the commonly used **PANI** dopant camphorsulfonic acid) or 2-naphthalene sulfonate ($C_{10}H_7SO_3^-$) may hinder the intermolecular stacking and thus obstruct the formation of the nanostructures (see Fig. S6, ESI†). These results are in agreement with the data obtained by Wang *et al.*[30]

3.1. Electrochemical properties of TANI nanowires

Fig. 4 shows the cyclic voltammogram obtained using a US-5M-modified CPE electrode. There are two reduction peaks at 0.145 V and 0.417 V *vs.* Ag/Ag^+, corresponding to the transitions from the emeraldine to leucoemeraldine and pernigraniline to emeraldine states of **TANI**, respectively.[31,32] The area under the CV curve of the US-5M-modified CPE electrode is much larger than that of the as-synthesized **TANI**-ES-modified CPE electrode, which indicates that US-5M samples may have a higher supercapacitive performance than **TANI**-ES. Detailed analysis is currently being performed to clarify the exact origin of this increased capacitance.

3.2. TANI nanowires assembled at different acid concentrations

According to the results obtained by Wang *et al.* in mixed solvent systems,[2] lower aqueous HCl concentrations (*e.g.* 0.1 M) lead to

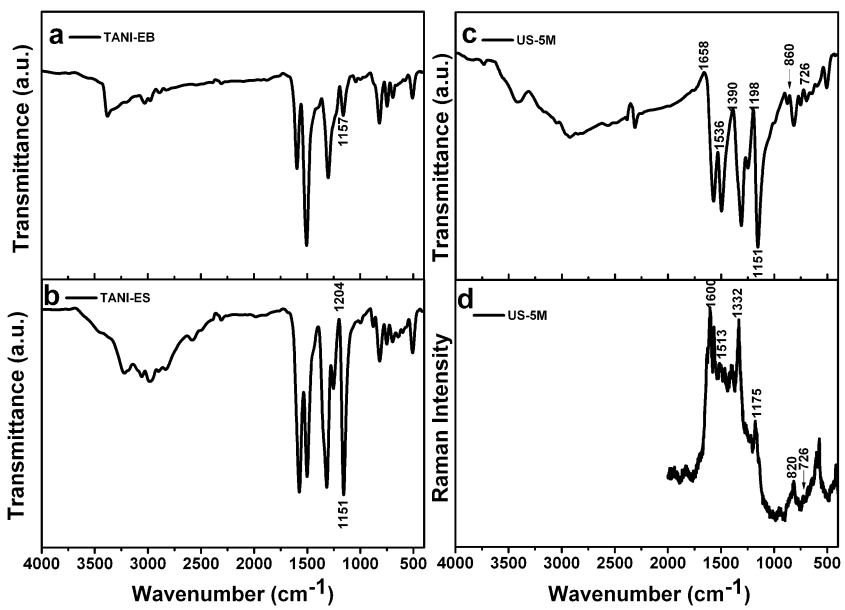

Fig. 3 Pellet (KBr) FTIR spectra of (a) **TANI**-EB, (b) **TANI**-ES, (c) US-5M samples and (d) Raman spectrum of US-5M.

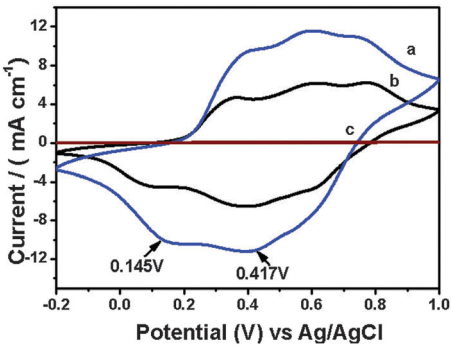

Fig. 4 Cyclic voltammetry curves (scan rate: 50 mV s^{-1}) of as-synthesized **TANI**-ES-modified CPE (a), US-5M-modified CPE (b) and bare CPE electrodes (c) in 1 M H_2SO_4.

individual nanowires, while increasing the concentration of HCl to 1 M will result in the formation of bundles of nanowires. To compare our results and gain further understanding of our less complex system (in addition to the US-5M system discussed so far), we also studied the structure and morphology of nanowires doped with different concentrations of aqueous HCl under ultrasonic irradiation (US-0.1M, US-1M, and US-7M, with the US-5M data included for ease of direct comparison).

The presence of nanowires is clearly observed for all the samples (Fig. 5). The images are presented in two magnifications (10 000× and 30 000×), where in the lower magnification it can be seen that the nanowire morphology is dominant. The average diameters of nanowires assembled from 0.1 M, 1 M, 5 M, and 7 M HCl in the higher magnification images are 49, 51, 47, and 39 nm, respectively. In particular, bundling and aggregation into thicker wires were observed for the US-1M and US-5M samples, with average bundle diameters of 130 nm and 120 nm, respectively.

The FT-IR spectra of US-0.1M, US-1M, US-5M, and US-7M samples show similar characteristics as already discussed for US-5M earlier, indicating the existence of extra hydrogen bonding ($NH^{+}\cdots N$) between neighbouring chains (Fig. S7, ESI†).[28] These hydrogen-bonding interactions, combined with the electrostatic interactions, might be the driving force for the self-assembly of

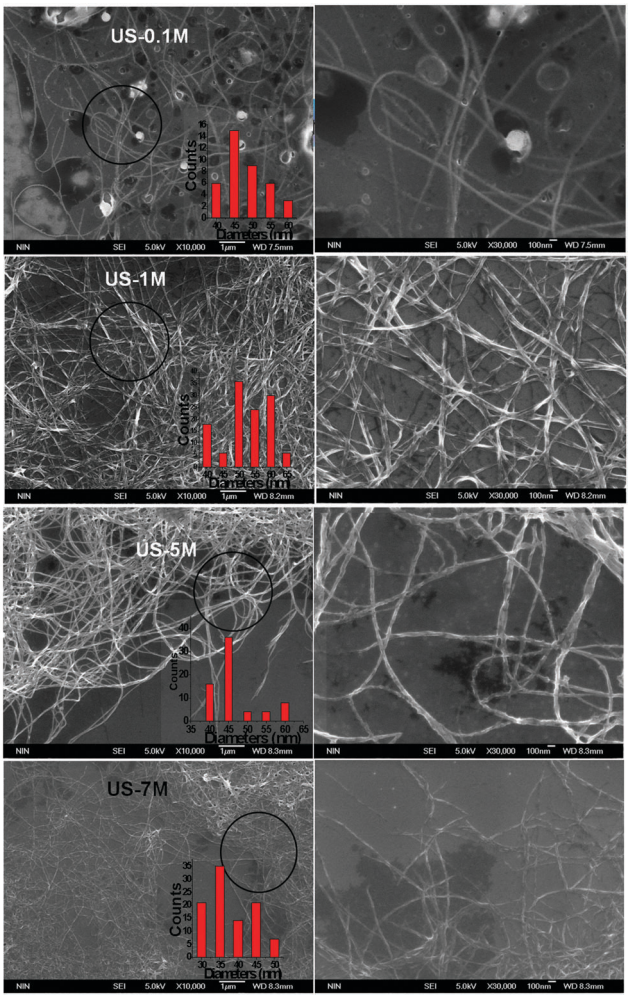

Fig. 5 SEM images of US-0.1M, US-1M, US-5M, and US-7M samples. Histogram values were obtained from the indicated circular areas by measuring the nanowire diameters at higher magnification.

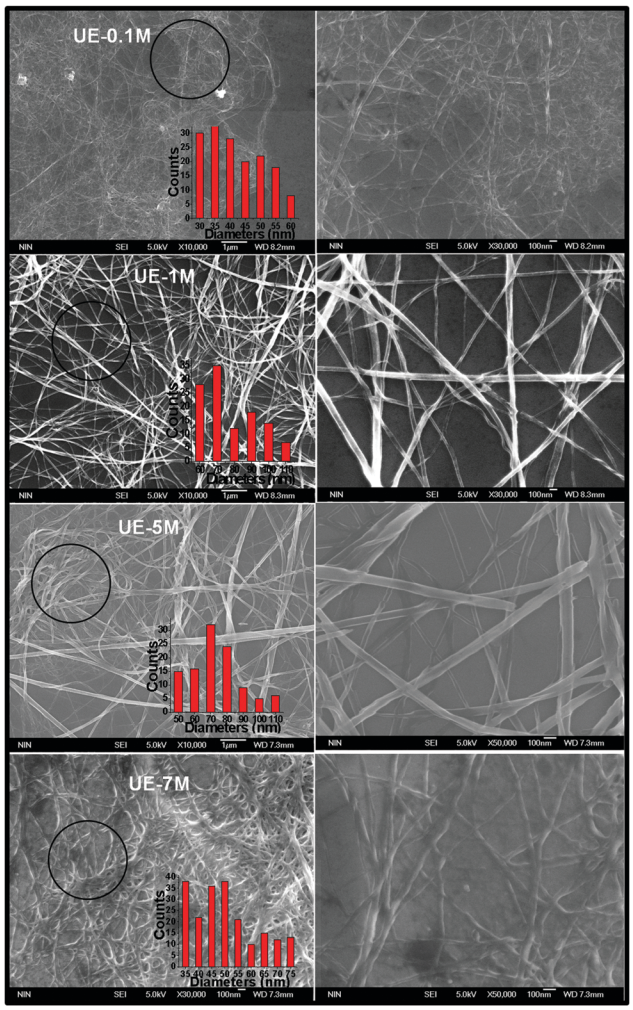

Fig. 6 SEM images of UE-0.1M, UE-1M, UE-5M, and UE-7M samples. Histogram values were obtained from the indicated circular areas by measuring the nanowire diameters at higher magnification.

the nanowires. As shown in the Table 1, the Cl/N ratio, which provides insight into the degree of doping, for US-1M and US-5M sample is higher than for the **TANI**-ES and US-0.1M samples, indicating optimal doping and thus also wire formation. Besides, with the increase in acid concentration, the excess protonic acid serves to screen charges and interactions,[33] and thus decreases the repulsive forces between molecules.[2] Therefore, for US-1M and US-5M samples, thicker nanowires were formed. When using a higher acid concentration (7 M HCl), the excess protonic acid leads to less effective protonation of the oligomer chains (as seen from the lowering of the Cl/N ratio).[34] In addition, TGA studies support the presented arguments, as US-1M and US-5M show increased stability and degradation temperatures over those with lower Cl/N ratios (Fig. S8, ESI†).

XRD patterns of US-0.1M, US-1M, US-5M and US-7M samples exhibit the expected and characteristic peaks, with the peak at $\sim 20^\circ$ 2θ ascribed to the periodicity parallel to the polymer chain and the peak at $\sim 25^\circ$ 2θ attributed to the periodicity perpendicular to the polymer chain (Fig. S9, ESI†).[35]

Table 2 The average diameters and conductivity values of different nanostructured **TANI**s doped with different HCl concentrations

	HCl concentration							
	0.1 M		1 M		5 M		7 M	
Samples	US-0.1M	UE-0.1M	US-1M	UE-1M	US-5M	UE-5M	US-7M	UE-7M
D (nm)	49	42	51	78	47	73	39	50
σ^a (mS cm^{-1})	19.4	25	49.6	103	43.6	98.1	30.6	39.93

[a] Measured in ambient air at 25 °C. The conductivity value of **TANI**-ES is 20.15 mS cm^{-1}.

3.3. Further self-assembly of TANI nanowires under quiescent conditions in acidic aqueous media

After ultrasonic irradiation, the samples were left undisturbed for 96 h. During this time, the nanowires further assembled into thicker structures to yield samples UE-01, UE-1M, UE-5M and UE-7M.

The self-assembled structures doped with different acid concentrations obtained under different conditions were compared, with SEM images obtained under quiescent conditions shown in Fig. 6. A general increase in the diameter is observed for the wires formed under quiescent conditions, as summarized in Table 2.

We used time-dependent UV-Vis spectroscopy to obtain further insight into this assembly process. UV-Vis spectra were collected 5 h into the process and then every 12 h until no further changes were detected in the relative peak ratios (Fig. 7). Two main bands located at 317 nm and 591 nm in the UV-Vis spectra of as-synthesized **TANI**-EB (Fig. 7c) are ascribed to π–π* transitions of the benzene ring and the benzenoid to quinoid (π_B–π_Q) excitonic transition. For the UE-5M nanowires, peaks at 290 nm, 420 nm and around 800 nm correspond to the typical π–π* transition, the polaron → π* and π → polaron band transitions, respectively,[1] indicating that the nanowires are in their doped and conductive emeraldine salt form. With the assembly process progressing, the ratio of the 420 nm peak to the 290 nm peak increases and the broad peak around 800 nm also increases in intensity compared to the peak at 290 nm. The changes in relative intensity of these peaks show that **TANI** molecules further assemble into the well-defined nanostructures through π–π stacking interactions.[1] The further assembly behaviour of **TANI** here in acidic media is similar to that observed in a binary solvent system in earlier published results.[1] The relative change of peaks located at 420 nm, 290 nm

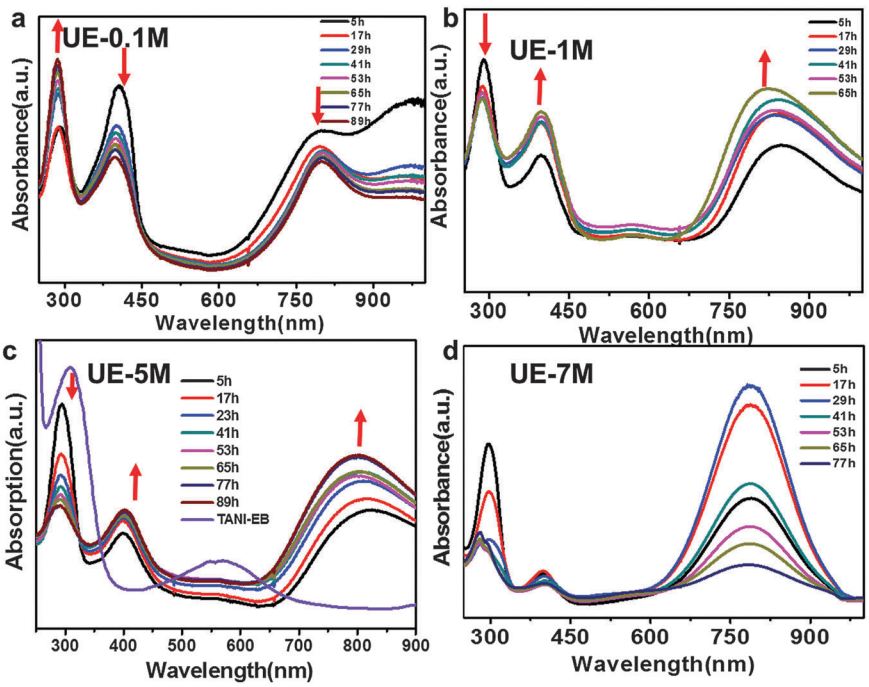

Fig. 7 UV-Vis spectra obtained at the given time intervals during the course of assembly of UE-0.1M (a), UE-1M (b), UE-5M (c) and UE-7M (d) samples.

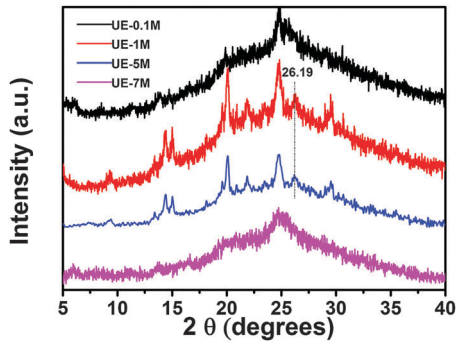

Fig. 8 XRD patterns of different UE-0.1M, UE-1M, UE-5M, and UE-7M samples. Peaks attributed to π-π stacking are indicated by the dotted line.

and the broad peak around 800 nm of the UE-1M sample is similar to that of the UE-5M sample. Moreover, the nanowires formed at high dopant concentration (7 M) tend to aggregate, with some dissolution of wires also observed with the passage of time. These changes are reflected as the emergence of two different bands at 300 nm after 29 h in the UV-Vis spectra of UE-7M sample shown in Fig. 7. It is noteworthy that the UV-Vis spectra of the doped low concentration sample, UE-0.1M, show additional absorbances beyond 1000 nm. With increasing dopant concentration, a clear progression can be seen up to the UE-7M sample, with no evidence of absorption at all in this higher wavelength region. This behaviour is similar to that observed by Kulszewicz-Bajer *et al.* in their detailed studies of lower aniline oligomers.[36,37]

The X-ray data for the UE sample series showed that the peak at $2\theta \approx$ *ca.* 10° is present for the UE-1M and UE-5M samples, indicating an increase of crystalline domain length (Fig. 8).[38] Furthermore, peaks at $2\theta \approx 26°$ for the different samples are attributed to classical π–π stacking between aromatic rings, and were observed in UE-1M and UE-5M samples (note that these reflections were absent or very ill-defined in the XRD data obtained after sonication). These data demonstrate that π–π stacking interaction contribute to the formation of well-defined nanostructures.[1] This stacking arrangement is also supported by the analysis of the UV-Vis spectra in Fig. 7.

3.4. Electronic transport properties of the obtained doped TANI nanowires

The conductivities of pressed pellets from the obtained **TANI** nanowires were determined by standard four-probe measurements. Previous studies on the conductivity of doped **TANI** measured on pressed pellets yielded conductivity values within the range of 10^{-5} to 10 mS cm^{-1}.[8,12,39] As shown in Table 2, as-synthesized **TANI**-ES has a conductivity of 20.15 mS cm^{-1}, while US-1M and US-5M nanowires have conductivities of 49.6 and 43.6 mS cm^{-1}, respectively. Moreover, the conductivities of UE-1M and UE-5M (*i.e.*, samples with well-defined nanowires) were 103 and 98.1 mS cm^{-1}, respectively, which is approximately 5-fold higher than that of as-synthesized **TANI**-ES. These measurements of conductivity (and thus functionality) indicate the advantage of self-assembled nanowires with well-defined π-stacked nanostructures for potential application.

4. Conclusion

We have shown here that the assembly of oligo(aniline)s in acidic aqueous media under ultrasonic irradiation yields well-defined nanowires over a range of acid concentrations. We deduce that the extra hydrogen bonding and electrostatic interaction associated with the protonation process drive the self-assembly of the nanowires, which is further influenced by intermolecular stacking. Careful choice of favourable routes to achieve thermodynamically stable systems, which include ultrasonic irradiation, assembly time and acid concentration (and thus degree of doping), is an important factor for promoting and controlling the assembly behaviour of oligo(aniline)s in acidic media. Additional control over functionality was also demonstrated, as reflected by significant enhancements in conductivity. These insights provide design rules for the rapid formation of anisotropic structures based on functional moieties whilst yielding enhanced conductivity. Further work in our laboratories, in addition to mechanistic studies, focuses on exploring anisotropic functionality of such assembled nanowire systems for applications in energy storage and sensing.

Acknowledgements

The authors gratefully acknowledge the National Natural Science Foundation of China (Grant No. 21307098), the Fundamental Research Founds for the Central Universities of China, and China Postdoctoral Science Foundation (2013 M532053). CFJF acknowledges the University of Bristol for support.

References

1 Y. Wang, H. D. Tran, L. Liao, X. Duan and R. B. Kaner, *J. Am. Chem. Soc.*, 2010, **132**, 10365.
2 Y. Wang, J. Liu, H. D. Tran, M. Mecklenburg, X. N. Guan, A. Z. Stieg, B. C. Regan, D. C. Martin and R. B. Kaner, *J. Am. Chem. Soc.*, 2012, **134**, 9251.
3 J. Feng and A. G. MacDiarmid, *Synth. Met.*, 1999, **102**, 1304.
4 Y. Wang, H. D. Tran and R. B. Kaner, *Macromol. Rapid Commun.*, 2011, **32**, 35.
5 Z. Shao, P. Rannou, S. Sadki, N. Fey, D. M. Lindsay and C. F. J. Faul, *Chem. – Eur. J.*, 2011, **17**, 12512.
6 Z. Yang, X. Wang, Y. Yang, Y. Liao, Y. Wei and X. Xie, *Langmuir*, 2010, **26**, 9386.
7 H. Kim, S. M. Jeong and J. W. Park, *J. Am. Chem. Soc.*, 2011, **133**, 5206.
8 S. P. Surwade, S. R. Agnihotra, V. Dua, N. Manohar, S. Jain, S. Ammu and S. K. Manohar, *J. Am. Chem. Soc.*, 2009, **131**, 12528.
9 H. Cui, Y. Liu, Y. Cheng, Z. Zhang, P. Zhang, X. Chen and Y. Wei, *Biomacromolecules*, 2014, **15**, 1115.
10 H. Cui, J. Shao, Y. Wang, P. Zhang, X. Chen and Y. Wei, *Biomacromolecules*, 2013, **14**, 1904.
11 C. U. Udeh, N. Fey and C. F. J. Faul, *J. Mater. Chem.*, 2011, **21**, 18137.

12 Z. Wei and C. F. J. Faul, *Macromol. Rapid Commun.*, 2008, **29**, 280.
13 Z. Shao, Z. Yu, J. Hu, S. Chandrasekaran, D. M. Lindsay, Z. Wei and C. F. J. Faul, *J. Mater. Chem.*, 2012, **22**, 16230.
14 Y. Zhao, E. Tomšík, J. Wang, Z. Morávková, A. Zhigunov, J. Stejskal and M. Trchová, *Chem. – Asian J.*, 2013, **8**, 129–137.
15 J. O. Thomas, H. D. Andrade, B. M. Mills, N. A. Fox, H. J. K. Hoerber and C. F. J. Faul, *Small*, 2015, **11**, 3430.
16 H. Huang, W. Li, H. Wang, X. Zeng, Q. Wang and Y. Yang, *ACS Appl. Mater. Interfaces*, 2014, **6**, 1595.
17 Y. Zhao, J. Stejskal and J. Wang, *Nanoscale*, 2013, **5**, 2620.
18 W. Lv, J. Feng, W. Yan and C. F. J. Faul, *J. Mater. Chem. B*, 2014, **2**, 4720.
19 W. Lv, J. Feng and W. Yan, *RSC Adv.*, 2015, **5**, 27862.
20 C. F. J. Faul, *Acc. Chem. Res.*, 2014, **47**, 3428.
21 O. A. Bell, J. S. Haataja, F. Broemmel, N. Fey, A. Seddon, R. R. Richardson, I. Ikkala, X. Zhang and C. F. J. Faul, *J. Am. Chem. Soc.*, 2015, **137**, DOI: 10.1021/jacs.5b06892.
22 Y. Li, W. He, J. Feng and X. Jing, *Colloid Polym. Sci.*, 2012, **290**, 817.
23 C. Park, H. J. Song and H. C. Choi, *Chem. Commun.*, 2009, 4803.
24 M. Sathish, K. i. Miyazawa, J. P. Hill and K. Ariga, *J. Am. Chem. Soc.*, 2009, **131**, 6372.
25 Y. Tao, Y. Shen, L. Yang, B. Han, F. Huang, S. Li, Z. Chu and A. Xie, *Nanoscale*, 2012, **4**, 3729.
26 K. S. Suslick, T. Hyeon and M. Fang, *Chem. Mater.*, 1996, **8**, 2172.
27 X. Lu, H. Mao, D. Chao, W. Zhang and Y. Wei, *Macromol. Chem. Phys.*, 2006, **207**, 2142.
28 P. Colomban, A. Gruger, A. Novak and A. Régis, *J. Mol. Struct.*, 1994, **317**, 261.
29 C. Laslau, Z. Zujovic and J. Travas-Sejdic, *Prog. Polym. Sci.*, 2010, **35**, 1403.
30 Y. Wang, H. D. Tran and R. B. Kaner, *J. Phys. Chem. C*, 2009, **113**, 10346.
31 S. Wang, D. Chao, E. B. Berda, X. Jia, R. Yang, X. Wang, T. Jiang and C. Wang, *RSC Adv.*, 2013, **3**, 4059.
32 D. Chao, S. Wang, R. Yang, E. Berda and C. Wang, *Colloid Polym. Sci.*, 2631, **201**, 291.
33 A. G. MacDiarmid and A. J. Epstein, *Synth. Met.*, 1994, **65**, 103.
34 G. M. do Nascimento, P. Y. G. Kobata and M. L. A. Temperini, *J. Phys. Chem. B*, 2008, **112**, 11551.
35 Q. Tang, J. Wu, X. Sun, Q. Li and J. Lin, *Langmuir*, 2009, **25**, 5253.
36 I. Kulszewicz-Bajer, I. Rozalska and M. Kurylek, *New J. Chem.*, 2004, **28**, 66.
37 I. Rozalska, P. Kulyk and I. Kulszewicz-Bajer, *New J. Chem.*, 2004, **28**, 1235.
38 J. P. Pouget, M. E. Jozefowicz, A. J. Epstein, X. Tang and A. G. MacDiarmid, *Macromolecules*, 1991, **24**, 779.
39 C. U. Udeh, P. Rannou, B. P. Brown, J. O. Thomas and C. F. J. Faul, *J. Mater. Chem. C*, 2013, **1**, 6428.

